RSC Advances

ROYAL SOCIETY OF CHEMISTRY

www.rsc.org/advances

RSC Advances RSC Publishing

PAPER

Microwave and Hydrothermal Synthesis of WSe_2 micro/nanorods and its Application in Supercapacitor

Cite this: DOI: 10.1039/x0xx00000x

Received 00th XXXXX 2014,
Accepted 00th XXXXX 2015

DOI: 10.1039/x0xx00000x

www.rsc.org/

Disha Chakravarty[1], Dattatray J. Late,[1]*

Abstract:

WSe_2 micro/nanorods were synthesized using one step microwave and hydrothermal method. The as synthesized micro/nanorod samples of WSe_2 were characterized by using various characterization techniques such as SEM, TEM, Raman spectroscopy, X-ray diffraction, UV-visible and PL spectroscopy. The as synthesized samples were also tested for their applicability to use as cathode materials for supercapacitor applications. The WSe_2 samples were prepared by microwave and hydrothermal (with use of tungstic acid as precursor) shows noteworthy performance towards supercapacitor application. Our work opens new avenue to use these simple methods to prepare various morphologies of inorganic nanomaterials and utilize them for various energy and nanoelectronics applications.

1. Introduction

Supercapacitors which are also known as the electrochemical capacitors are considered as the essential power source due to promising energy-storage device applications. The important parameters of these devices are high power densities, rate of charge/discharge, life cycle stability, durability and low cost. Owing to these remarkable properties, the researcher has been accepted to the area of supercapacitors, to fabricate electrode using various nanomaterials for advanced energy storage devices. Over the past few years, there has been remarkable growth in various perspectives of engineering applications of one-dimensional (1D) and two-dimensional (2D) inorganic oxide layered materials especially transition metal dichalcogenides[1-7] such as MoS_2 [8–24],WS_2 [25–28],$MoSe_2$[29–32], WSe_2[33–39], GaS[15,40], GaSe[15, 40] and other 2D insulating[41-44] and oxide materials [45, 46] have attracted much attention from scientific community due to their extraordinary electrical, optical and magnetic properties. Among all, the WSe_2 layered materials in 1D nanometric form has not yet been widely investigated for energy storage and other applications due to difficulties in the synthesis and other related issues. The 2D form of WSe_2 has been recently reported as field effect transistors [8–13], photodetectors[16], for photocatalytic hydrogen production[47] in solar cells[48–50]and heterostructures[11]. The bulk WSe_2 is a layered semiconductors with indirect bandgaps ~1.21 eV[51], in monolayer form it exhibits direct bandgaps of 1.67 eV[52]. The WSe_2 belong to

transition metal dichalcogenides (TMDCs) crystal structure made up of hexagonal layers of metal atoms (M= Mo, W, V, Ga, Ta, Sn) sandwiched in between two layers of chalcogen atoms (X = S, Se, Te)[8-24]. The WSe_2 is a naturally occurring metal selenide with intriguing electronic, electrochemical and electrocatalytic properties, formed by 2D covalently bonded Se−W−Se layers separated by a van der Waals gap. The WSe_2 possesses hexagonal crystal structure with space group P63/mmc and each WSe_2 monolayer contains an individual layer of W atoms with 6-foldcoordination symmetry, which is hexagonally packed between two trigonal atomic layers of Se atoms.

The atomically thin layered WSe_2 has attracted much attention for the diverse applications in nanoelectronic devices because of its suitable wide and direct band gap[53]. It is possible that the layered WSe_2 can offer easy electron transport through MX_2 nanostructures, which gives high specific capacitance values by faster ion diffusion between the layers as reported for other TMDCs [54-55]. Graphene and its composite with other materials have been utilized for its suitability for supercapacitors applications [54-55]. Moreover it is important that for high performance supercapacitor, material should have properties such as high power density, fast power delivery or uptake, and excellent cycle-to-cycle stability etc. These properties are essential for material to be used in high performance energy storage devices [56-61]. The TMDCs materials like MoS_2 and WS_2 has been recently reported for their supercapacitor behaviour[54-55], but WSe_2, which is also belongs to the same layered chalcogenide family has not yet been explored till date for its application as supercapacitor.

In the present investigations, we report synthesis of WSe_2 nanorods and nanoparticles using simple microwave assisted route and hydrothermal method and its supercapacitor behaviour. The WSe_2 exhibited enhanced and stable supercapacitive behaviour in three electrode capacitance measurement geometry.

Results and discussion:

The WSe_2 samples were prepared by using three different routes. Here after the sample prepared by microwave-assisted method were named as WSe_2-A, next the sample prepared by using hydrothermal method using tungstic acid and elemental selenium salts were called as WSe_2-B and finally the sample prepared by using hydrothermal method with ammonium tungstate and elemental selenium salts were called as WSe_2-C. Here after samples were described by above nomenclature. Fig. 2(a-d) shows the typical SEM images of WSe_2-A sample prepared using microwave method depicts the rod like morphology of with typical dimension 10-80 µm in length and 1-2 µm in diameter. Fig. 3(a-d) shows the typical TEM images of WSe_2-A sample, depicting rods like morphology. Fig. 3(e-f) shows HR-TEM images of the WSe_2-A sample showing the good quality of the samples prepared using microwave route. The inset of Fig. 3(f) shows the typical diffraction pattern of WSe_2-A sample, showing hexagonal structure and highly oriented along <001>axis. Fig. 4(a) shows the typical XRD pattern of WSe_2-A sample, which matches well with the JCPDS data card No 06-0080.The sample also shows some other phases in addition to WSe_2 which indicates that our sample is slightly impure. This needs additional details X-ray photoelectron spectroscopy and other investigations. The WSe_2-A sample prepared using microwave method has been further characterized by using Raman spectroscopy as shown in Fig. 4(b).The typical Raman spectra of WSe_2-A sample excited using a 514.5 nm laser source shows bands at A_{1g}-LA (135 cm^{-1}), E^1_{2g} (247 cm^{-1}), A_{1g} (255 cm^{-1}) modes. It has been reported that the A_{1g} and E^1_{2g} bands of single-layer WSe_2 are separated by ~ 11 cm^{-1} [54].The light absorption properties of the as-synthesized WSe_2-A sample were characterized by using the UV-Vis absorption spectra. Fig. 4(c)

shows the UV-Vis absorption spectra of WSe_2-A. The absorption of the WSe_2-A was extended to the UV region. From the optical absorption spectra, it is evident that the WSe_2-A showed absorption onset of 220 nm.The room temperature PL spectrum of WSe_2-A sample were shown in Fig. 4(d). It exhibits a strong PL peak at ~ 728 nm.

The supercapacitive performances of WSe_2-A samples were measured in a three-electrode system in the 0.5 M KOH aqueous electrolyte. The specific capacitances of WSe_2 electrode has been calculated from the following equation.

$$\mathrm{Csp}\ (\mathrm{F/g}) = \frac{1}{2\mathrm{m}v(v2 - v1)} \int_{v1}^{v2} \mathrm{I}(v)\ \mathrm{d}v$$

Where m is the mass of single electrode material, v is the scan rate (mV/s), v1 and v2 are the integration limits (potential window), and I(v) denotes the response current (A). The capacitive performance of WSe_2-A was measured in a three-electrode system in the 0.5 M KOH aqueous electrolyte. Fig. 5(a) shows the comparative cyclic voltammograms (CVs) of WSe_2-A at different scan rate. The CV curve consist of area under curve which shows the charge storage capacity of the electrode therefore the value of specific capacitance calculated at a scan rate 100 mV/s is found to be 1.939 F/g. Fig. 5(b) shows the typical comparative charge–discharge profiles of WSe_2-A at current density of 1 and 5μA. Fig. 5(c) depicts the single charging-discharging cycle for the 400 cycles. The electron/ion transport at electrode/electrolyte interface and charge transfer resistance (R_{ct}) is further investigated by electrochemical impedance spectroscopy (EIS) techniques, the Warburg impedance can be determined using the straight line inclined to the real axis [62]. The slope of the Warburg impedance depicts the diffusion of electrolyte into the electrodes. The R_{ct} values of WSe_2-A samples were measured in 0.5 KOH at10.0 Ω which is shown in Fig. 5(d).

Fig. 6(a-e) shows the typical SEM images of WSe_2-B sample depicting micro-rods like morphology which is similar to the WSe_2-A, with dimensions 10-90 μm length and 1-2 μm diameters. Fig. 7(a-c) shows typical TEM images of WSe_2-B sample and Fig.7(d) shows the typical SAED pattern of the sample representing the single crystalline nature of WSe_2-B sample. Fig. 8(a) shows the typical XRD pattern of WSe_2-B which matches with the JCPDS data card no. 06-0080. Fig. 8(b) depicting the typical Raman spectra of the WSe_2-B sample which matches with reported spectra in the litrature[56]. The light absorption study was carried out using the UV-Vis absorption spectra and is shown in Fig. 8(c). The absorption of the WSe_2-B was observed in UV region and the absorption onsets of 220 nm were noted. The PL spectrum of WSe_2-B sample is taken at room temperature as shown in Fig. 8(d). It exhibits a strong PL peak centred at 728 nm. The capacitive performance of WSe_2-B was also investigated in a three-electrode system in the 0.5 M KOH aqueous electrolyte. Fig. 9(a) shows the comparative cyclic voltammograms (CVs) of WSe_2-B sample at different scan rate. The area under the CV curve represents the charge storage capacity of the electrode therefore the value of specific capacitance calculated at a scan rate100 mV/s is found to be 2.44 F/g. The Comparative charge–discharge profiles of the WSe_2-B at different current densities are showed in Fig. 9(b). The Fig. 9(c) depicts the single charging-discharging cycle from the 400 cycles which is shown in Fig. 9(d).The R_{ct} values of WSe_2-B nanorods were measured in 0.5 KOH at 11.0 Ω.

Fig. 10(a-f) shows the typical SEM images of WSe_2-C sample, showing micron size particle like morphology with dimension 2-5 μm which were further observed to be decorated with small nanoparticle on the micron size particle. Fig. 11(a-b) depicts the typical TEM images of WSe_2-C sample, which shows well uniform growth of particle like morphology. Fig. 11(c-d) shows HR-

TEM images of WSe_2-C sample shown in high resolution. The crystal qualities of the samples were analysed using diffraction pattern which is shown in the inset of Fig. 11(d). The Fig. 12 (a) shows the typical XRD pattern of WSe_2-C sample confirming the high quality of the as synthesized sample. The WSe_2-C sample was further examined by Raman spectroscopy. Fig. 12(b) shows the Raman spectra of WSe_2-C matches very well with the earlier results in this manuscript. The light absorption characteristics were examined by using UV-Vis absorption spectra which is shown in Fig. 12(c). The absorption of WSe_2-C sample was characterized using UV the absorption with observed onset was of 220 nm. The WSe_2-C sample were further, characterized by using PL spectrum at room temperature, it exhibits a strong PL peak centred at 727.9 nm depicts in Fig. 12(d). The capacitive performance of WSe_2-C was also measured in a three-electrode system in the 0.5 M KOH aqueous electrolyte. Fig. 12(a) shows the comparative cyclic voltammograms (CVs) of WSe_2-C at different scan rate. The area under the CV curve represents the charge storage capacity of the electrode therefore the value of specific capacitance calculated at a scan rate 100 mV/s is found to be 2.44 F/g. Fig. 13(b) shows the typical comparative charge–discharge profiles of both the samples at different current density. Fig. 13(c) depicts the single charging-discharging cycle from the 400 cycles. Fig. 13(d) shows impedance spectra of WSe_2-C. The results typically consist of a curve at high frequencies and a straight line at lower frequencies. The R_{ct} values of WSe_2-C were measured in 0.5 KOH at 37.0 Ω. Fig. 13(e) shows the comparative CVs of all three sample WSe_2-A, WSe_2-B and WSe_2-C at 100 mV/s and Fig. 13(f) depicts the comparative charge-discharge profile at same current density of 5A. The Table 1 summarize the results of supercapacitor performance of different voltage sweep rates (50, 100, 200, 500, and 1000 mV/s) on the specific capacitance which was examined for all three samples of WSe_2.

Conclusions:

In conclusion, we have synthesized WSe_2 micro/nanorod using two different methods namely one step microwave and hydrothermal method. We have also successfully synthesized WSe_2 micro/nano-particle covered with small WSe_2 naoparticles (size ~ 100 nm) using hydrothermal method. In addition to pure phase some impurities in the sample also noted, which need further detail investigations. The samples were tested for its suitability to use in supercapacitor applications. The WSe_2 micro-rod prepared using microwave and hydrothermal method shows better performance towards cyclic stability and good performance towards charging and discharging cycle. Impedance spectroscopy results of all samples reveal that a lower R_{ct} value and thicker electrical double layers formations are responsible for its superior capacitive behaviour. Our results opens new avenue to prepare WSe_2 and various other inorganic layered materials using simple hydrothermal and microwave method and use novel morphologies of these materials for energy applications including supercapacitor to replace the conventional batteries.

Experimental Section:

(a) Microwave synthesis of WSe_2Nanorods

The WSe_2 microrods were synthesized by two methods. First it was synthesized by the one step microwave-assisted method. In the typical microwave reaction the stoichiometry quantities of the precursor powders elemental selenium (2 mM) and Ammonium tungstate (1mM) and sodium borohydrate (3 mM) were dissolved in 10 mL ethylene glycol followed by purging inert N_2 gas for a few minutes prior to switching on the microwave. The microwave-assisted reaction was carried out in a Spectra 750 W microwave oven, with a 2.45 GHz working frequency. The oven was modified to include a refluxing system. During the experiments, the

microwave oven was operated for switching on for 30 s and off for next 15 s, with use of total power ~750 W upto 3 minutes. For the post reaction, the product was centrifuge using ethanol solvent for several at 4500 rpm followed by washing using DI water and drying in vacuum for 3 hours.

(b) Hydrothermal synthesis of WSe_2 Microrods

Second method for WSe_2 microrod synthesis was hydrothermal reaction. In a typical reaction, we used 1g of ammonium tungstate[$(NH_4)10H_2(W_2O_7)_6$, 0.89g of elemental selenium and 8 mL of hydrazine monohydrate were added in 25 mL capacity of teflon-lined stainless steel autoclave and distilled water were filled 80% of the total volume of autoclave.

(c) Hydrothermal synthesis of WSe_2 Nanoparticles

The third method to synthesize WSe_2 nanostructure were the same hydrothermal method with different source of tungsten as tungstic acid were used. In hydrothermal method, the typical preparation temperature was maintained at 150-170 ^{0}C for 48 h. For the post reaction autoclaves were cooled naturally followed by washing with distils water and ethanol successively and then final product was dried under vacuum at 50^{0}C for 2 h.

(d) Characterization:

All WSe_2 samples were further characterized by using several analytical tools such as XRD, Raman, SEM, TEM, UV-Vis and PL etc. The crystallographic structures and phase confirmation of WSe_2 samples were analysed by X-ray diffraction (XRD, Philips powder diffractometer PW3040/60 with Cu Kα radiation). Scanning electron microscopy (SEM) images were acquired using FEI ESEM QUANTA 200 3D instrument. High resolution-transmission electron microscopy (HR-TEM) images were obtained using FEI TECNAI TF-30 (FEG) instrument. The Raman spectra were recorded at room temperature, with a (LabRAM HR) using Ar laser (514.5 nm) in the back scattering geometry. The adsorption capacity of samples was analysed by HORIBA Flurolog 3 spectroflurometer instrument. The photoluminescence is measured by exciting the samples with 400 nm solid-state laser of few milliwatt.

Acknowledgements

Dr. D. J. Late would like to thank Department of Science and Technology (Government of India) for Ramanujan Fellowship (Grant No. SR/S2/RJN-130/2012).The research work was primarily supported by NCL-MLP project grant 028626, DST-SERB Fast-track Young scientist project Grant No. SB/FT/CS-116/2013 and the partial support by INUP IITB project sponsored by DeitY, MCIT.

Notes and references

Physical & Materials Chemistry Division, CSIR-National Chemical Laboratory, Dr. Homi Bhabha Road, Pune 411008, Maharashtra, India.
Email: dj.late@ncl.res.in / datta099@gmail.com

[1] S.V. Morozov, A. K. Geim, *Proc. Nat. Acad. Sci*. 2005,**102**,10451.
[2] K. S. Novoselov, A. K. Geim, S. V. Morozov, D. Jiang, Y. Zhang, S. V. Dubonos, I. V. Grigorieva, A. A. Firsov, *Science* , 2004,**306**, 666.
[3] K. S. Novoselov, A. K.Geim, S.V. Morozov, D. Jiang, M. I. Katsnelson, I.V. Grigorieva, S.V. Dubonos, A. A. Firsov, *Nature*, 2005, **438**,197.
[4] F. Schwierz, *Nat. Nanotech*.2010, **5**, 487.
[5] A. Ghosh, D. J. Late, L.S. Panchakarla, A. Govindaraj, C. N. R. Rao, *J. Exp. Nanosci.,*2009, **4,** 313.
[6] D. J. Late, U. Maitra, L. S. Panchakarla, U. V. Waghmare, C. N. R. Rao,*J. Phys.: Condens. Matter*, 2011,**23**, 055303.
[7] F. Schedin, A. K. Geim, S. V. Morozov, E. W. Hill, P. Blake, M. I. Katsnelson, K. S. Novoselov, *Nat. Mater.* 2007, **6**, 652.
[8] B. Radisavljevic, A. Radenovic, J. Brivio, V. Giacometti, A. Kis, *Nat. Nanotechnol*. 2011, **6**, 147.

[9] D. J. Late, P. A. Shaikh, R. Khare, R. V. Kashid, M. Chaudhary, M. A. More, S. B. Ogale, ACS Appl. Mater. Interfaces 2014, **6**, 15881.

[10] D. J. Late, B. Liu, H. S. S. R. Matte, V. P. Dravid, C. N. R. Rao, *ACS Nano* 2012, **6**, 5635.

[11] K. Roy, M. Padmanabhan, S. Goswami, T. P. Sai, G. Ramalingam, S. Raghavan, A. Ghosh, *Nat. Nanotechnol.* 2013, **8**, 826.

[12] H. Wang, L. Yu, Y. Lee, Y. Shi, A. Hsu, M. L. Chin, L. Li, M. Dubey, J. Kong, T. Palacios, *NanoLett*. 2012, **12**, 4674.

[13] D. Jariwala, V. K. Sangwan, D. J. Late, J. E. Johns, V. P. Dravid, T. J. Marks, L. J. Lauhon, M. C. Hersam, *Appl. Phys. Lett.* 2013, **102**, 173107.

[14] H. S. S. R. Matte, A. Gomathi, A. K. Manna, D. J. Late, R. Datta, S. K. Pati, C. N. R. Rao, *Angew. Chem. Int. Ed*. 2010, **122**, 4153.

[15] D. J. Late, B. Liu, H. S. S. R. Matte, C. N. R. Rao, V. P. Dravid, *Adv. Funct. Mater*. 2012, **22**, 1894.

[16] Z. Yin, H. Li, H. Li, L. Jiang, Y. Shi, Y. Sun, G. Lu, Q. Zhang, X. Chen, H. Zhang, *ACS Nano* 2012, **6**, 74.

[17] A. Castellanos-Gomez, N. Agrat, G. Rubio-Bollinger, *Appl. Phys. Lett.*2010, **96**, 213116.

[18] R. V. Kashid, D. J. Late, S. S. Chou, Y. Huang, M. De, D. S. Joag, M. A. More, V. P. Dravid, *Small* 2013, **9**, 2730.

[19] Q. Zhang, H. Zhang, *Small* 2012, **8**, 63.

[20] D. J. Late, Y. Huang, B. Liu, J. Luo, J. Acharya, S. N. Shirodkar, J. Luo, A. Yan, D. Charles, U. V. Waghmare, V. P. Dravid, C. N. R. Rao, *ACS Nano* 2013, **7**, 4879.

[21] F. K. Perkins, A. L. Friedman, E. Cobas, P. M. Campbell, G. G. Jernigan, B. T. Jonker, *NanoLett.* 2013, **13**, 668.

[22] C. Lee, H. Yan, L. E. Brus, T. F. Heinz, J. Hone, S. Ryu, *ACS Nano* 2010, **4**, 2695.

[23] J. D. Lin, C. Han, F. Wang, R. Wang, D. Xiang, S. Qin, X. Zhang, L. Wang, H. Zhang, A. T. S. Wee, W. Chen,ACS Nano 2014, **8**, 5323.

[24] Y. Shi, J. Huang, L. Jin, Y. Hsu, S. F. Yu, L. Li, H. Y. Yang, *Sci. Rep.* 2013, **3**, 1839.

[25] D. Braga, I. G. Lezama, H. Berger, A. F. Morpurgo, *NanoLett*. 2012, **12**, 5218.

[26] T. Georgiou, R. Jalil, B. D. Belle, L. Britnell, R. V. Gorbachev, S. V. Morozov, Y. J. Kim, A. Gholinia, S. J. Haigh, O. Makarovsky, L. Eaves, L. A. Ponomarenko, A. K. Geim, K. S. Novoselov, A. Mishchenko, *Nat. Nanotechnol*. 2013, **8**, 100.

[27] A. Berkdemir, H. R. Guti_rrez, A. R. Botello-Mendez, N. Perea Lpez, A. L. Elas, C.-I. Chia, B. Wang, V. H. Crespi, F. Lpez-Uras, J. C. Charlier, H. Terrones, M. Terrones, *Sci. Rep.* 2013, **3**, 1755.

[28] N. Perea-Lopez, A. L. Elas, A. Berkdemir, A. Castro-Beltran, H. R. Guti_rrez, S. Feng, R. Lv, T. Hayashi, F. L_pez-Uras, S. Ghosh, B. Muchharla, S. Talapatra, H. Terrones, M. Terrones, *Adv. Funct. Mater.* 2013, **23**, 5511.

[29] S. Tongay, J. Zhou, C. Ataca, K. Lo, T. S. Matthews, J. Li, J. C. Grossman, J. Wu, *Nano Lett.* 2012, **12**, 5576.

[30] J. S. Ross, S. Wu, H. Yu, N. J. Ghimire, A. M. Jones, G. Aivazian, J. Yan, D. G. Mandrus, D. Xiao, W. Yao, X. Xu, *Nat. Commun.* 2013, **4**, 1474.

[31] S. Larentis, B. Fallahazad, E. Tutuc, *Appl. Phys. Lett*. 2012, **101**, 223104.

[32] D. J. Late, T. Doneux, M. Bougouma, Appl. *Phys. Lett.* 2014, **105**, 233103.

[33] H. Fang, S. Chuang, T. C. Chang, K. Takei, T. Takahashi, A. Javey, *NanoLett.* 2012, **12**, 3788.

[34] W. Liu, J. Kang, D. Sarkar, Y. Khatami, D. Jena, K. Banerjee, *NanoLett.* 2013, **13**, 1983.

[35] H. Sahin, S. Tongay, S. Horzum, W. Fan, J. Zhou, J. Li, J. Wu, F. M. Peeters, *Phys. Rev. B* 2013, **87**, 165409.

[36] Y. Zhao, X. Luo, H. Li, J. Zhang, P. T. Araujo, C. K. Gan, J. Wu, H. Zhang, S. Y. Quek, M. S. Dresselhaus, Q. Xiong, *NanoLett.* 2013, **13**, 1007.

[37] A. M. Jones, H. Yu, N. J. Ghimire, S. Wu, G. Aivazian, J. S. Ross, B. Zhao, J. Yan, D. G. Mandrus, D. Xiao, Y. Yao, X. Xu, *Nat. Nanotechnol*. 2013, **8**, 634.

[38] H. Yuan, M. S. Bahramy, K. Morimoto, S. Wu, K. Nomura, B. Yang, H. Shimotani, R. Suzuki, M. Toh, C. Kloc, X. Xu, R. Arita, N. Nagaosa, Y. Iwasa, *Nat. Phys.* 2013, **9**, 563.

[39] J.K. Huang, J. Pu, C.-L. Hsu, M.H. Chiu, Z.-Y. Juang, Y.-H. Chang, W.-H. Chang, Y. Iwasa, T. Takenobu, L.-J. Li, *ACS Nano*, 2014, **8**, 923.

[40] D. J. Late, B. Liu, J. Luo, A. Yan, H. S. S. R. Matte, M. Grayson, C. N. R. Rao, V. P. Dravid, *Adv. Mater.* 2012, **24**, 3549.

[41] A. Pan, Y. Chen, J. Li, CrystEngComm. 2015, **4**, 1539.

[42] C. R. Dean, A. F. Young, I. Meric, C. Lee, L. Wang, S. Sorgenfrei, K. Watanabe, T. Taniguchi, P. Kim, K. L. Shepard, J. Hone, *Nat. Nanotechnol.* 2010, **5**, 722.

[43] H. Zeng, C. Zhi, Z. Zhang, X. Wei, X. Wang, W. Guo, Y. Bando, D. Golberg, *NanoLett.* 2010, **10**, 5049.

[44] L. Song, L. Ci, H. Lu, P. B. Sorokin, C. Jin, J. Ni, A. G. Kvashnin, D. G. Kvashnin, J. Lou, B. I. Yakobson, P. M. Ajayan, *NanoLett.* 2010, **10**, 3209.

[45] S. Balendhran, S. Walia, M. Alsaif, E. P. Nguyen, J. Z. Ou, S. Zhuiykov, S. Sriram, M. Bhaskaran, K. Kalantar-zadeh, *ACS Nano* 2013, **7**, 9753.

[46] S. Balendhran, S. Walia, M. Alsaif, E. P. Nguyen, J. Z. Ou, S. Zhuiykov, S. Sriram, M. Bhaskaran, K. Kalantar-zadeh, *ACS Nano*, 2013,7, 9753.

[47] Y. Li, Y.-L. Li, C. M. Araujo, W. Luo, R. Ahuja, *Catal. Sci. Technol.* 2013, **3**, 2214.

[48] M. Shanmugam, C. A. Durcan, B. Yu, *Nanoscale* 2012, **4**, 7399.

[49] M. Bernardi, M. Palummo, J. C. Grossman, *NanoLett.* 2013, **13**, 3664.

[50] X. Gu, W. Cui, H. Li, Z. Wu, Z. Zeng, S. Lee, H. Zhang, B. Sun, *Adv. Energy Mater.* 2013, **3**, 1262.

[51] R. Coehoorn, C. Haas, R. A. de Groot, *P*hysical *Review B.*1987, **35**,6203.

[52] H. Terrones, F. Lo´pez-Urı´as, M. Terrones, *Scientific Reports*, 2013, **3**, 1549.

[53] L. Cao, S. Yang, W. Gao, Z. Liu, Y. Gong, L. Ma, G. Shi, S. Lei, Y. Zhang, S. Zhang, R. Vajtai, P. M. Ajayan, *Small* 2013, **9**, 2905.

[54] D. Hanlon, C. Backes, T. M. Higgins, M. Hughes, A. O'Neill, P. King, et al. *Chem Mater* 2014, **26**, 1751.

[55] S. Ratha, C. S. Rout. *ACS Appl Mater Interfaces* 2013, **5**, 11427.

[56] D. J. Late, S. N. Shirodkar, U. V. Waghmare, V. P. Dravid, C. N. R. Rao. *ChemPhysChem* 2014, **15**, 1592.

[57] C. S. Rout, P. D. Joshi, R.V. Kashid, D. S. Joag, M. A. More, A. J. Simbeck, M. Washington, S. K. Nayak, D. J. Late. *Sci .Rep. Uk* 2013, **3**, 3282.

[58] H. X. Chang , H. K Wu. *Energ Environ Sci* 2013, **6**, 3483.

[59] H. T. Zhang, X. Zhang, X. Z Sun, D. C. Zhang, H. Lin, C. H. Wang, H. Wang, Y. Ma. *Chemsuschem* 2013, **6**, 1084.

[60] B. Zhang, R. Shi, Y. P. Zhang, C. X. Pan. *Prog Nat Sci-Mater* 2013, **23**, 164.

[61] D. Yu , K. Goh , L. Wei , H. Wang , Q. Zhang , W. Jiang , R. Si , Y. Chen , *J. Mater. Chem. A.* 2013 , **1** , 11061.

[62] Q.Wang, J. E. Moser, M. Gratzel. *J PhysChem B* 2005, **109**,14945-53.

RSC Advances RSC Publishing

PAPER

Figure 1:

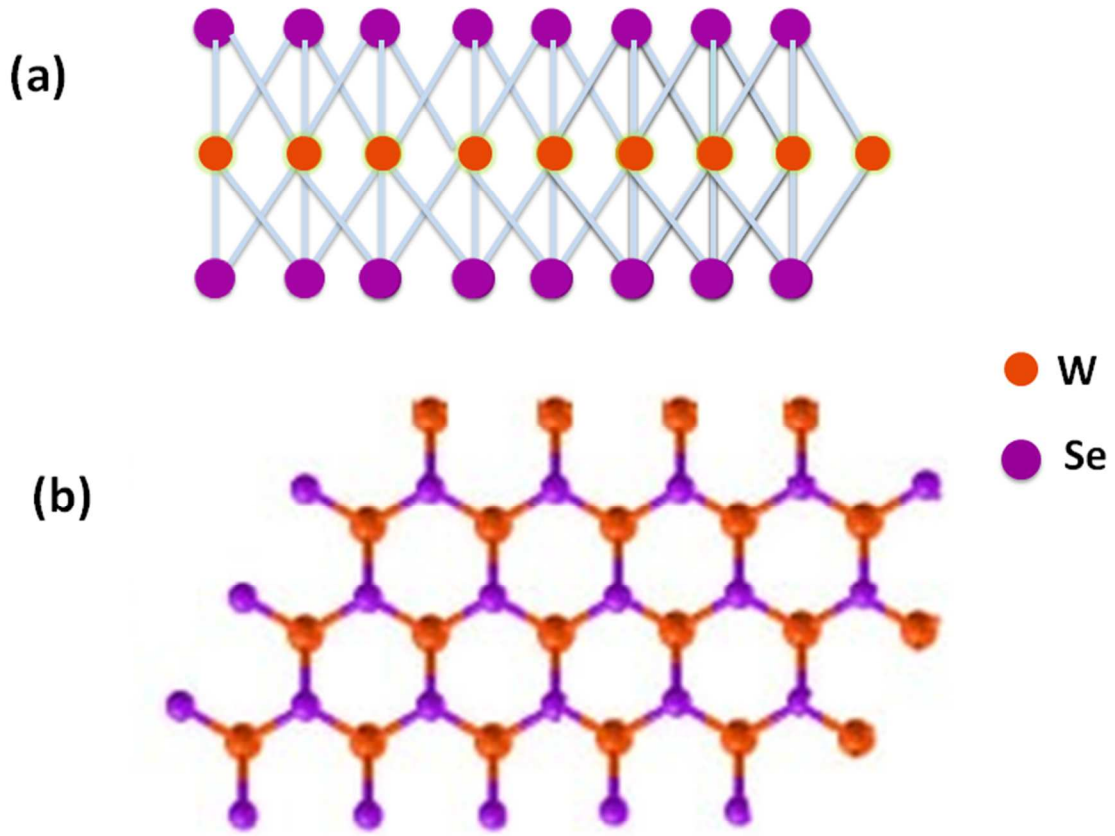

Fig.1: Schematic of WSe_2 structure (a) side view and (b) top view.

Figure 2:

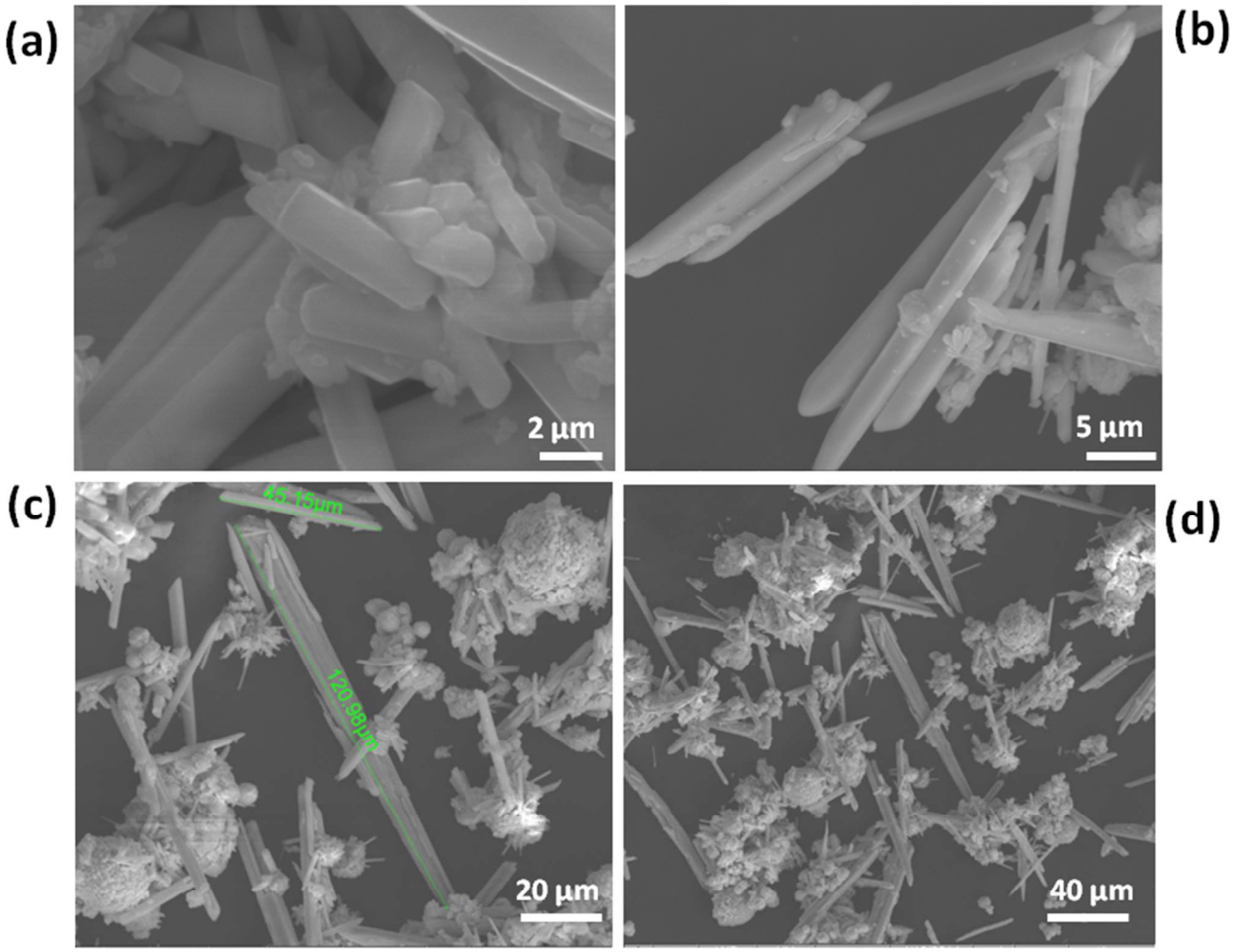

Fig. 2 :(a-d)SEM images of WSe_2 –A synthesized by microwave method by using ammonium molybadate salt.

Figure 3:

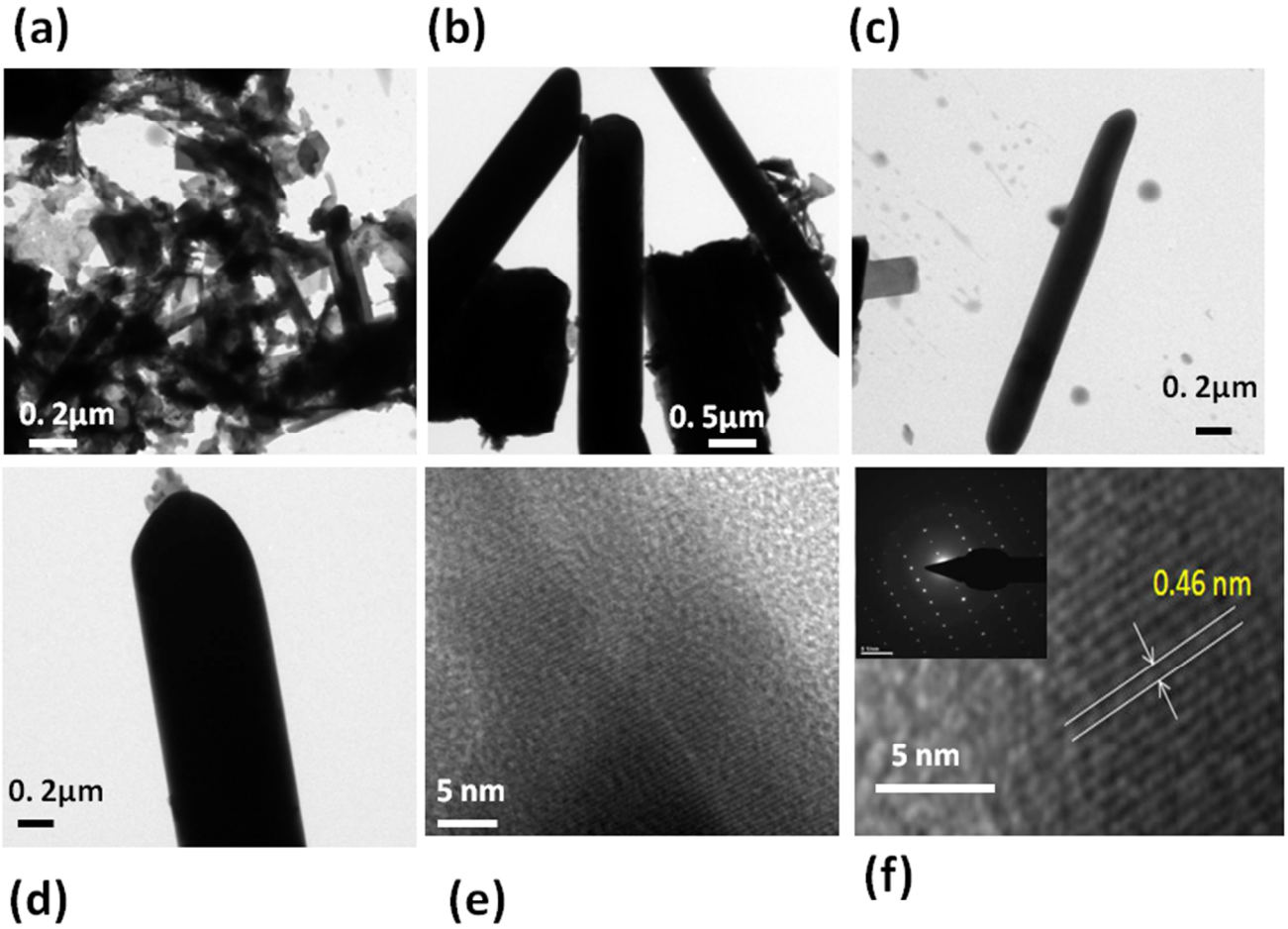

Fig. 3: (a-d) TEM images of WSe_2 synthesized by microwave method. (e-f) HRTEM images and inset of (f) shows the typical SAED pattern showing high crystalline quality of the as synthesized sample.

Figure 4:

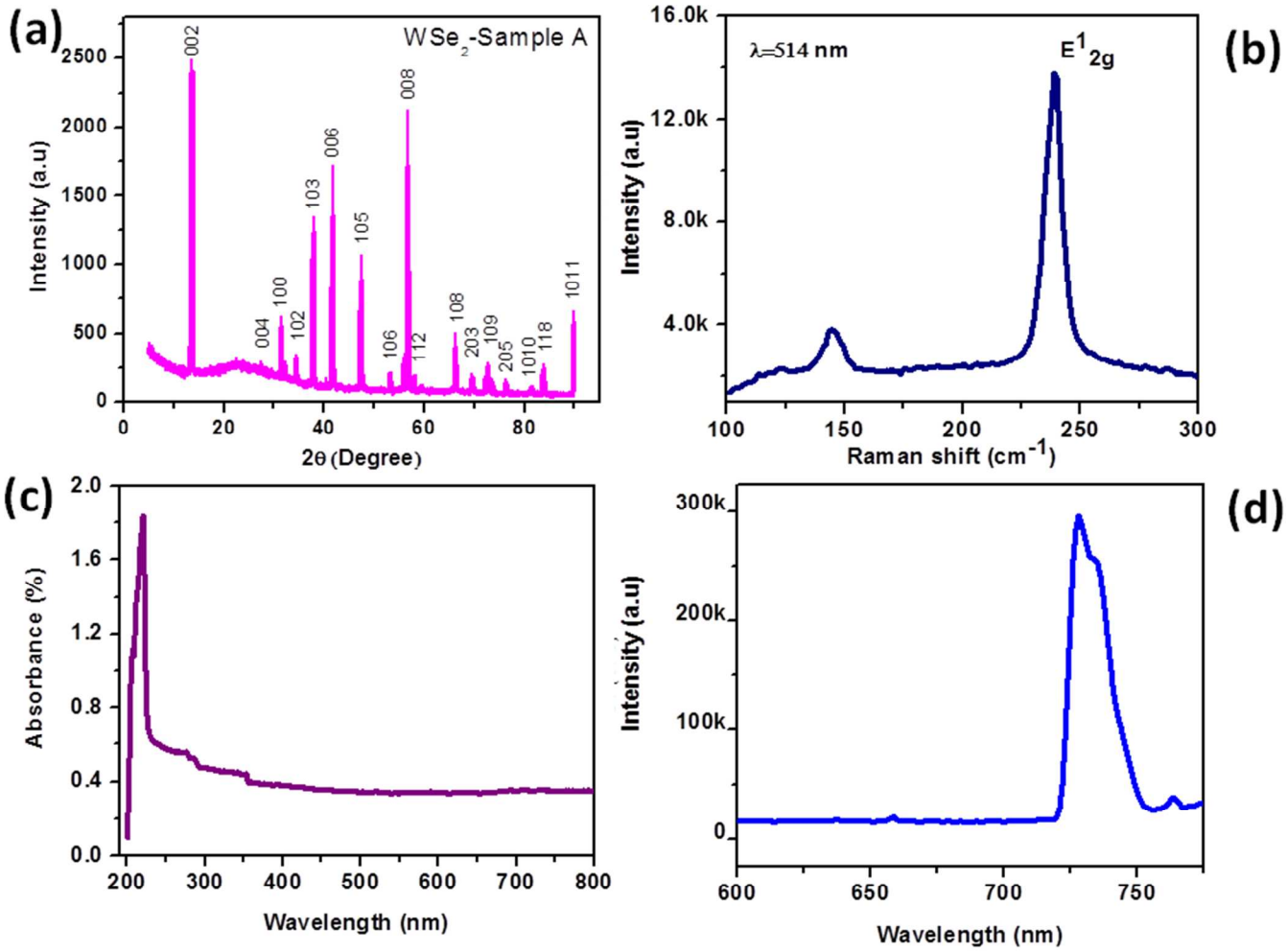

Fig. 4: WSe_2 microroad sample synthesized by Microwave method (a) XRD (b) Raman Spectra, (c) UV-visible spectra and (d) PL spectra.

Figure 5:

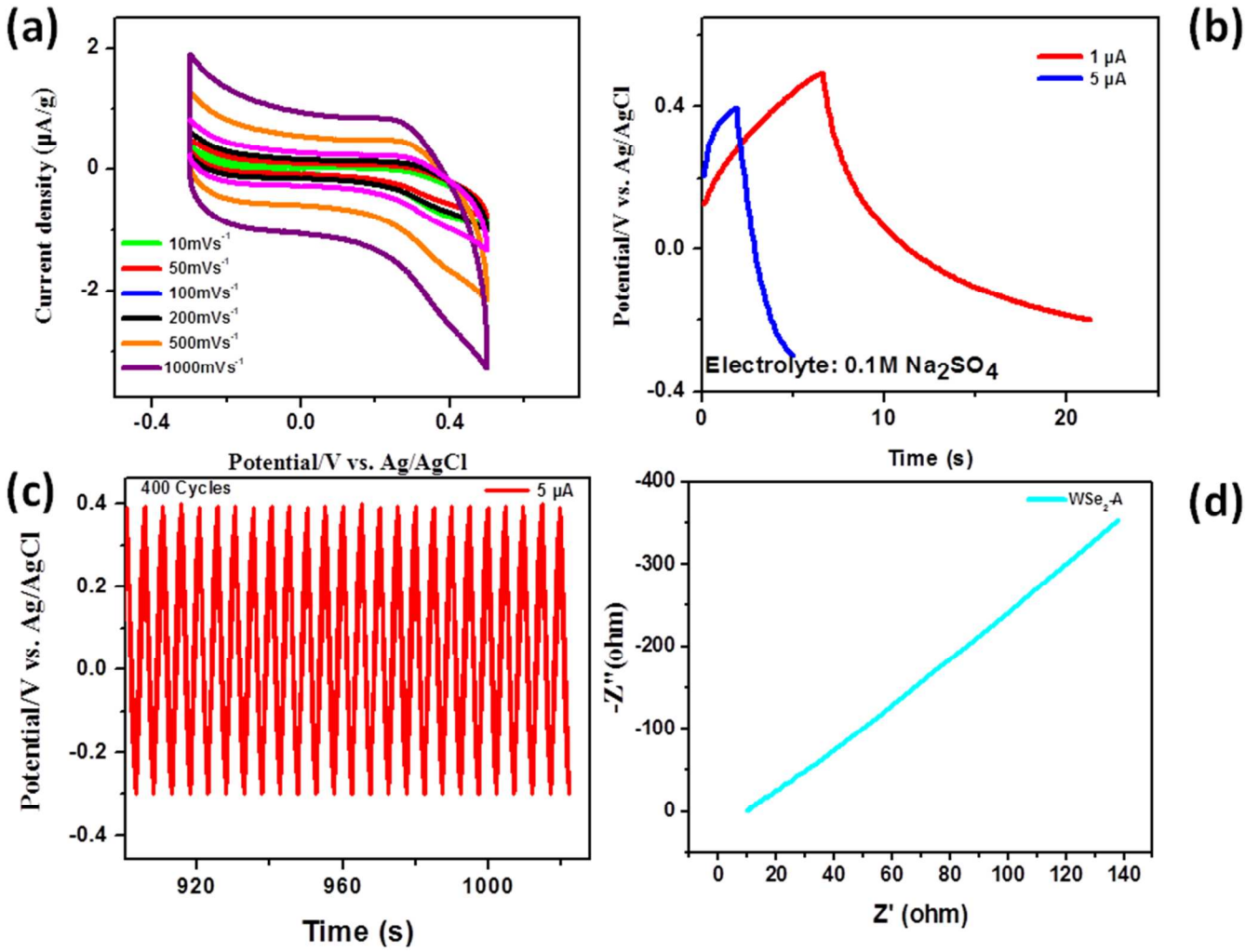

Fig. 5: Supercapacitor based on WSe_2 micro rod synthesized by microwave method.(a) Cyclic voltogramm at different scan rate, (b) Charging-discharging profile at different current density., (c) Charging-discharging profile for 400 cycles and (d) impedance spectroscopy.

Figure 6:

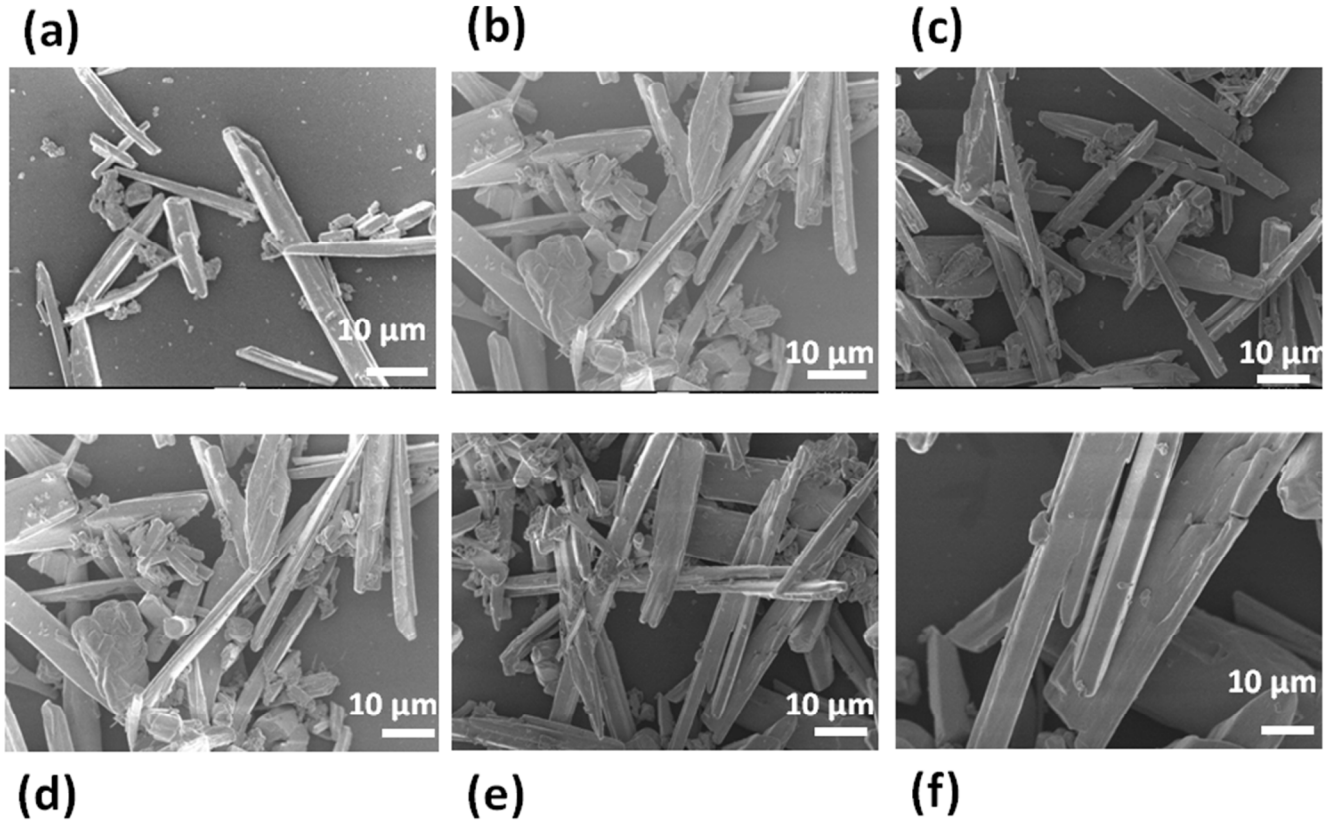

Fig. 6: (a-f) SEM images of WSe_2 microrod synthesized by hydrothermal method by using tungstic acid as source material.

Figure 7:

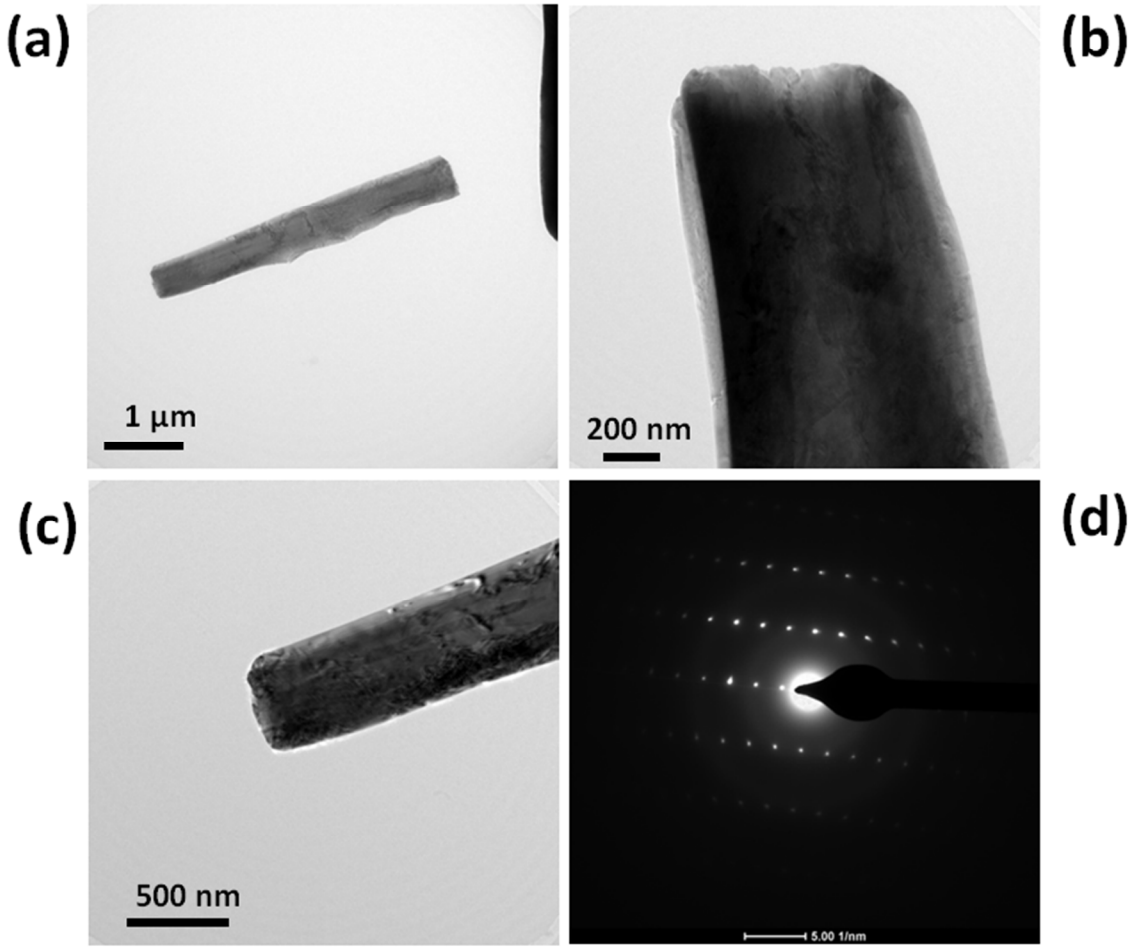

Fig. 7: (a-c) TEM images of WSe_2 microrod synthesized by hydrothermal method and (d) Typical SAED pattern of WSe_2 micro/nano rod sample.

Figure 8:

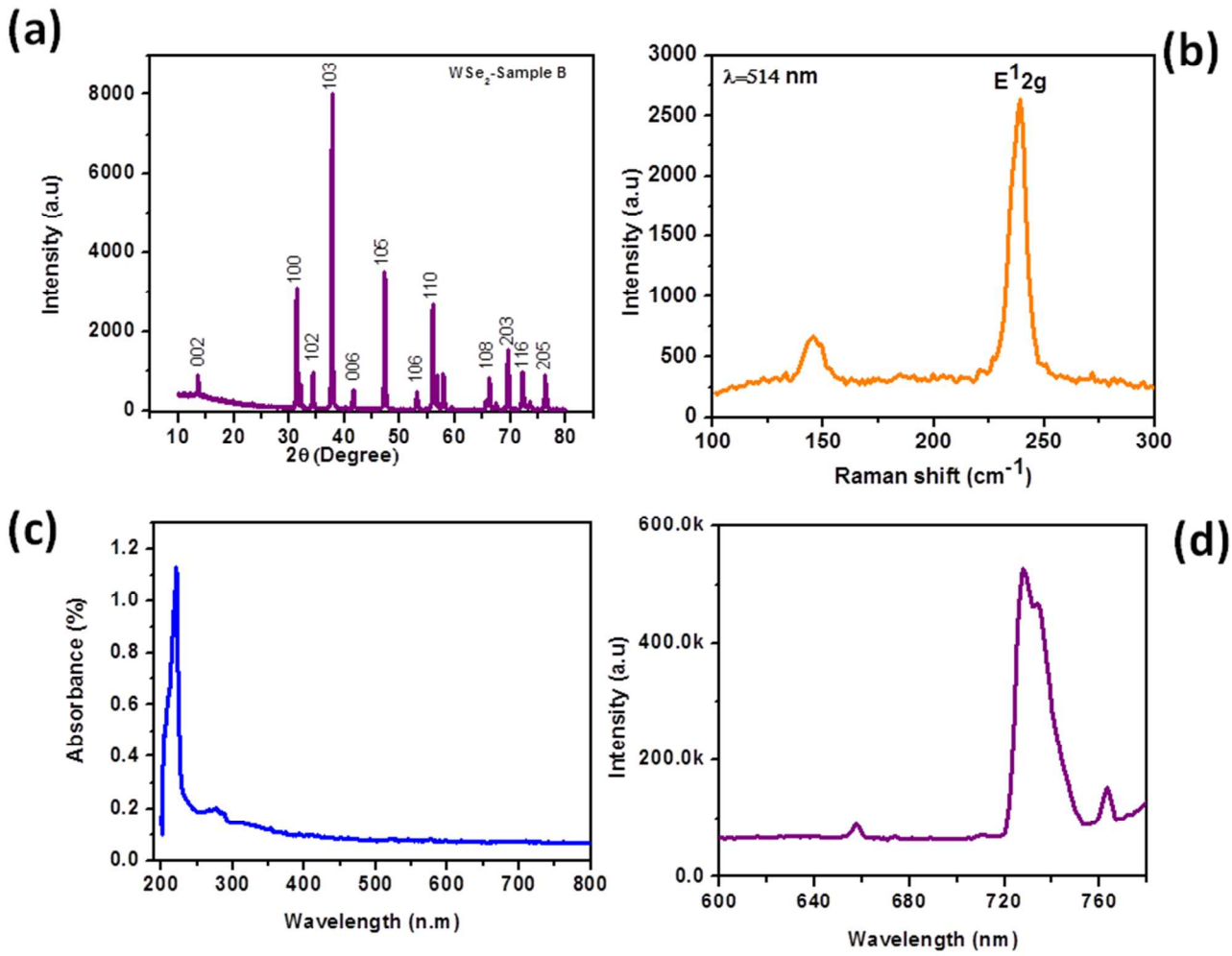

Fig. 8: WSe_2 micro/nano rods synthesized by hydrothermal method by using tungstic acid as source.(a) XRD pattern (b) Raman Spectra (c) UV-Visible spectra and (d) PL spectra.

Figure 9:

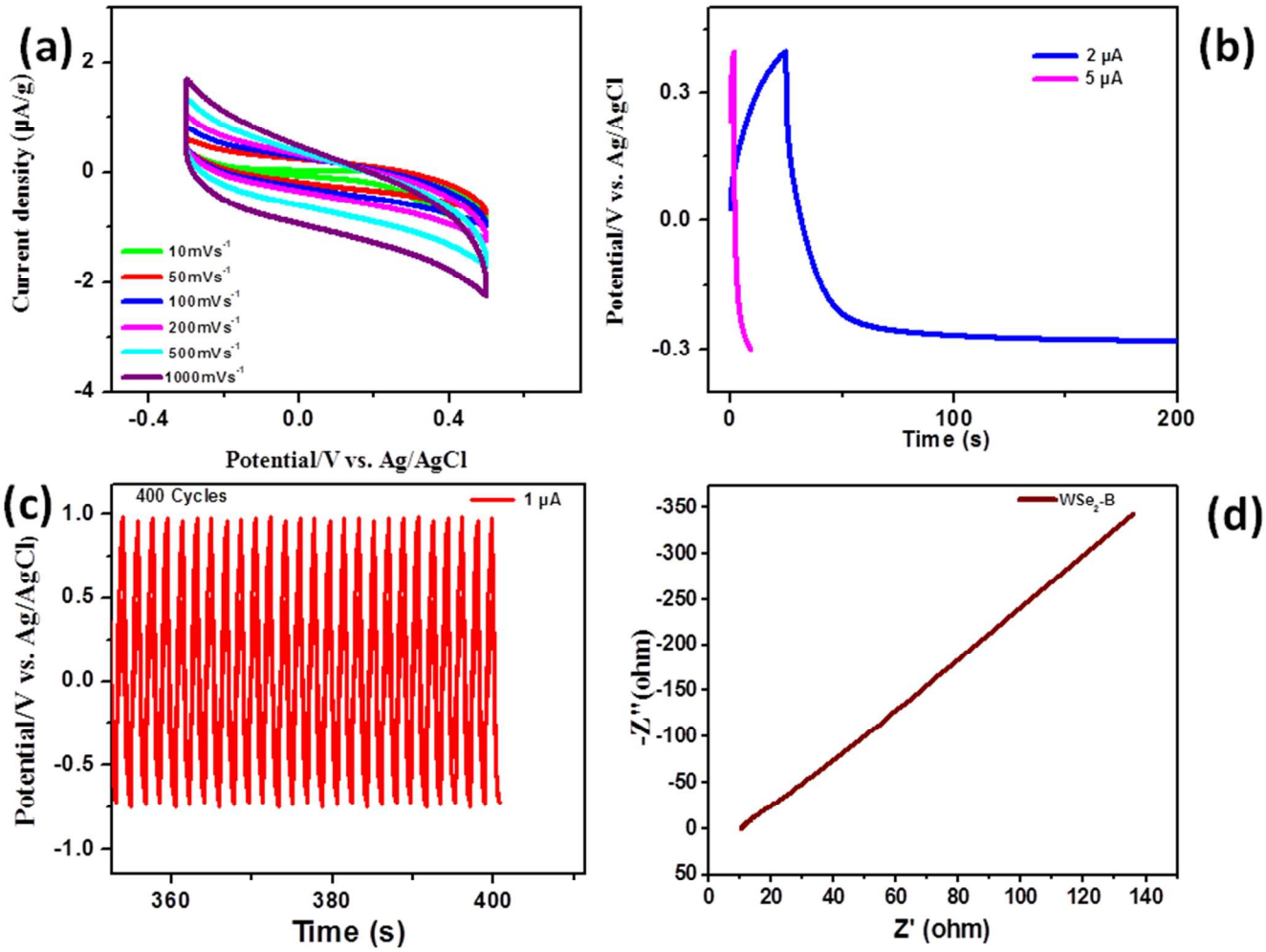

Fig. 9: Supercapacitor based on WSe_2 micro/nano road sample synthesized by hydrothermal method by using tungstic acid as source: (a) Cyclic voltogramm at different scan rate, (b) Charging-discharging profile at different current density., (c) Charging-discharging profile for 400 cycles and (d) impedance spectroscopy.

Figure 10:

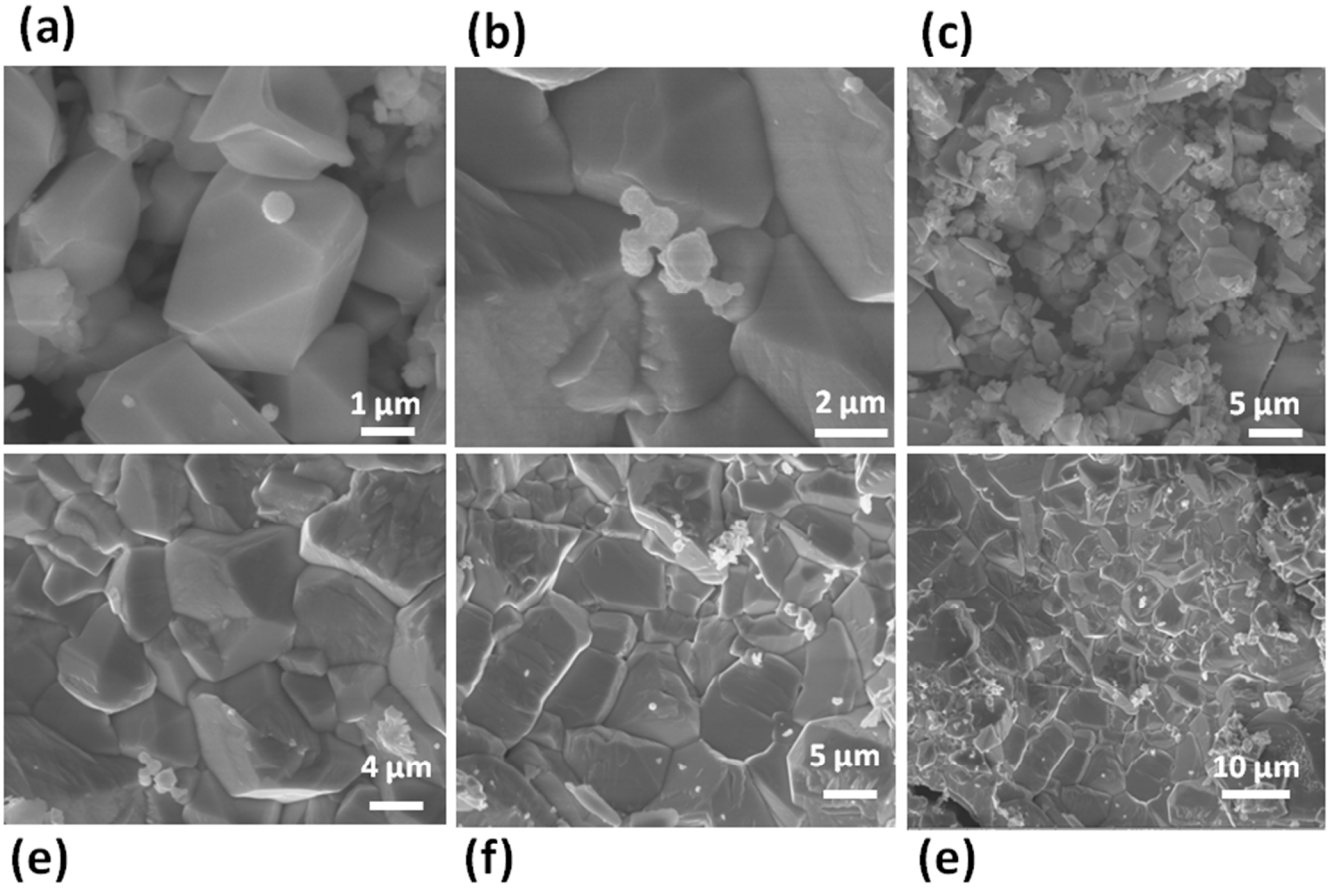

Fig. 10: (a-f) SEM images of WSe_2 micro /nano particles synthesized by hydrothermal method by using ammonium molybadate as source material.

Figure 11:

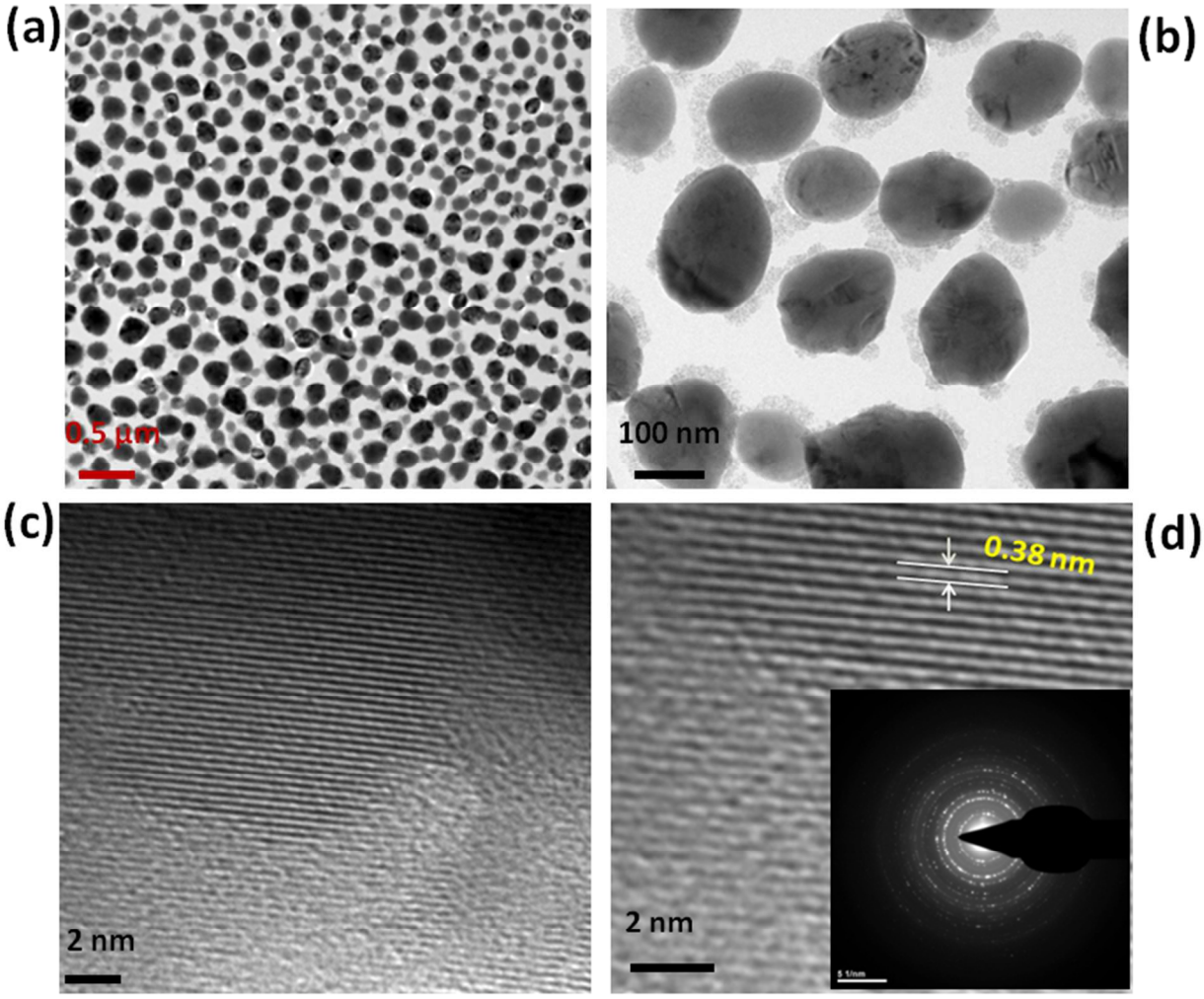

Fig. 11: WSe_2 micro /nanoparticles synthesized by hydrothermal method by using ammonium molybadate as source: (a-b) TEM images, (c-d) HR-TEM images. Inset of (d) shows the typical SAED pattern of WSe_2 micro /nano particles.

Figure 12:

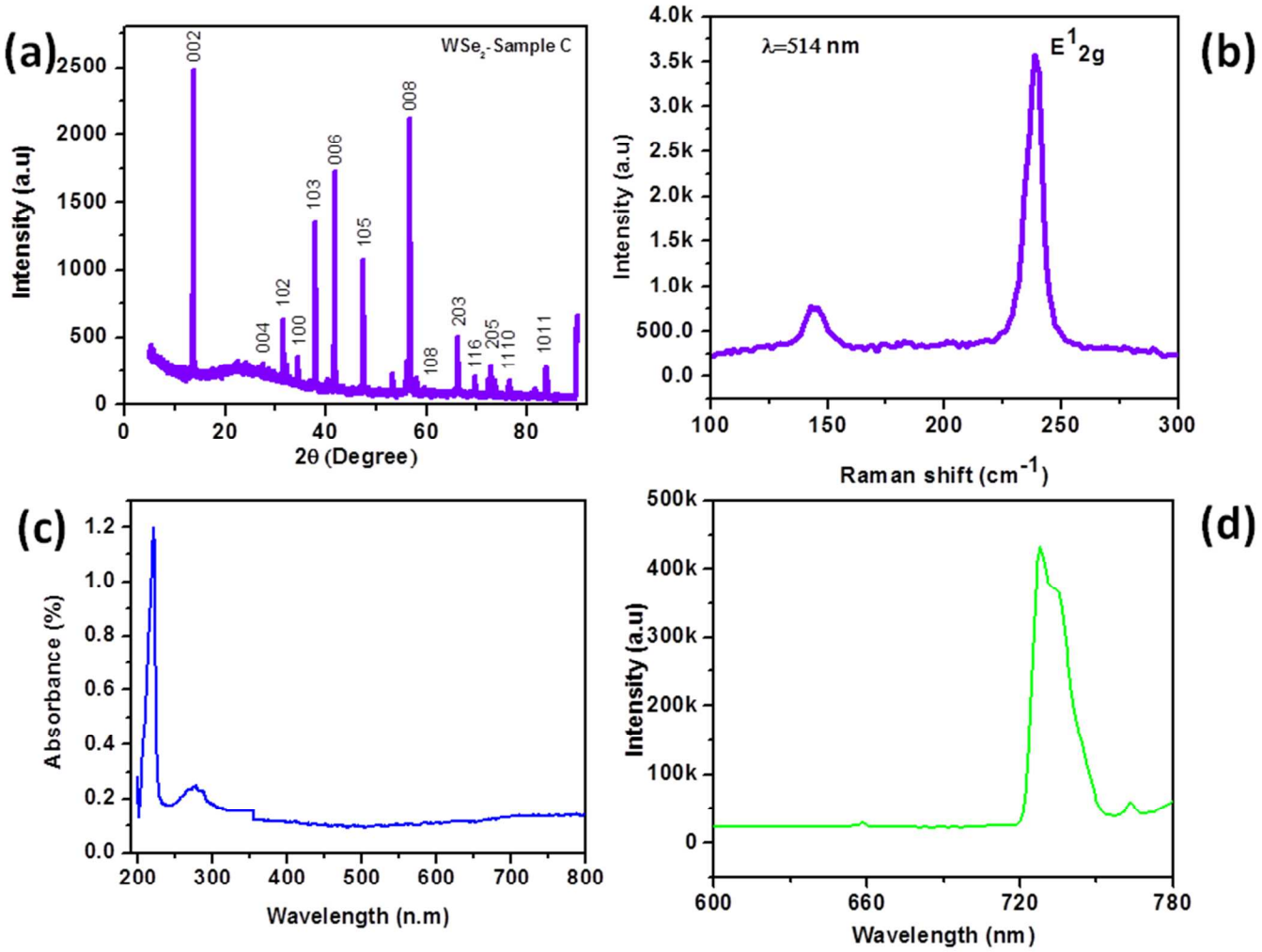

Fig. 12: WSe_2 micro/nano particles synthesized by hydrothermal method using ammonium molybadate as source materials: (a) XRD pattern (b) Raman Spectra (c) UV-Visible spectra (d) PL spectra.

Figure 13:

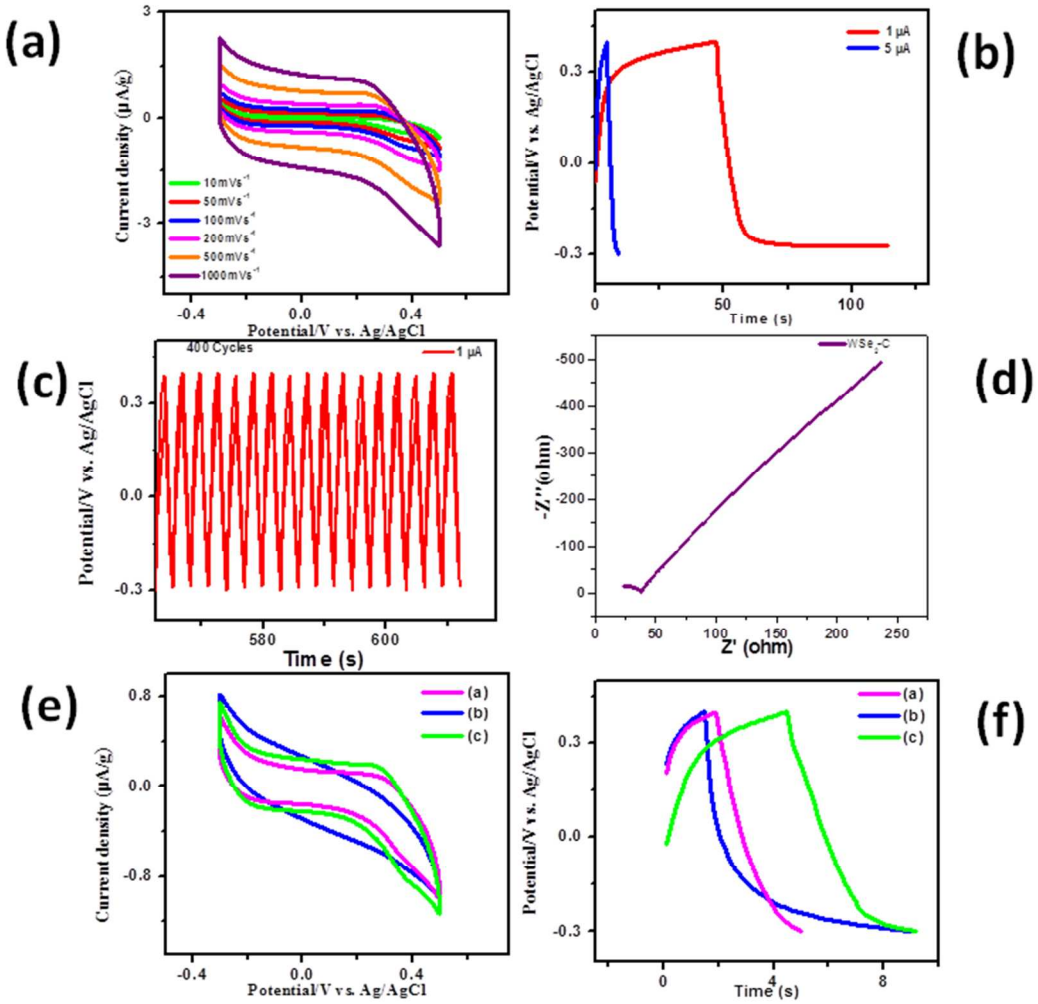

Fig. 13: Supercapacitor based on WSe_2 micro/nanoparticles synthesized by hydrothermal method by using ammonium molybadate. (a) Cyclic voltogramm at different scan rate, (b) Charging-discharging profile at different current density, (c) Charging-discharging profile for 400 cycles and (d) impedance spectroscopy. (e,f) shows the comparative study of WSe_2-A, WSe_2-B and WSe_2-C sample for Cyclic voltogramm at 100 $mVs^{-1}$and charge-discharge profile at current density of 5 μA respectively.

Table 1:

Sample	Voltage scan rate 10 mVs^{-1}	Voltage scan rate 50 mVs^{-1}	Voltage scan rate 100 mVs^{-1}	Voltage scan rate 200 mVs^{-1}	Voltage scan rate 500 mVs^{-1}	Voltage scan rate 1000mVs^{-1}
WSe_2-A	10.41	2.48	1.939	1.58	1.26	1.06
WSe_2-B	10.41	3.76	2.44	1.50	0.88	0.64
WSe_2-C	6.125	3.19	2.59	2.12	1.61	1.28

Table 1: Specific capacitance for all samples of WSe_2 at different scan rate.

TOC:

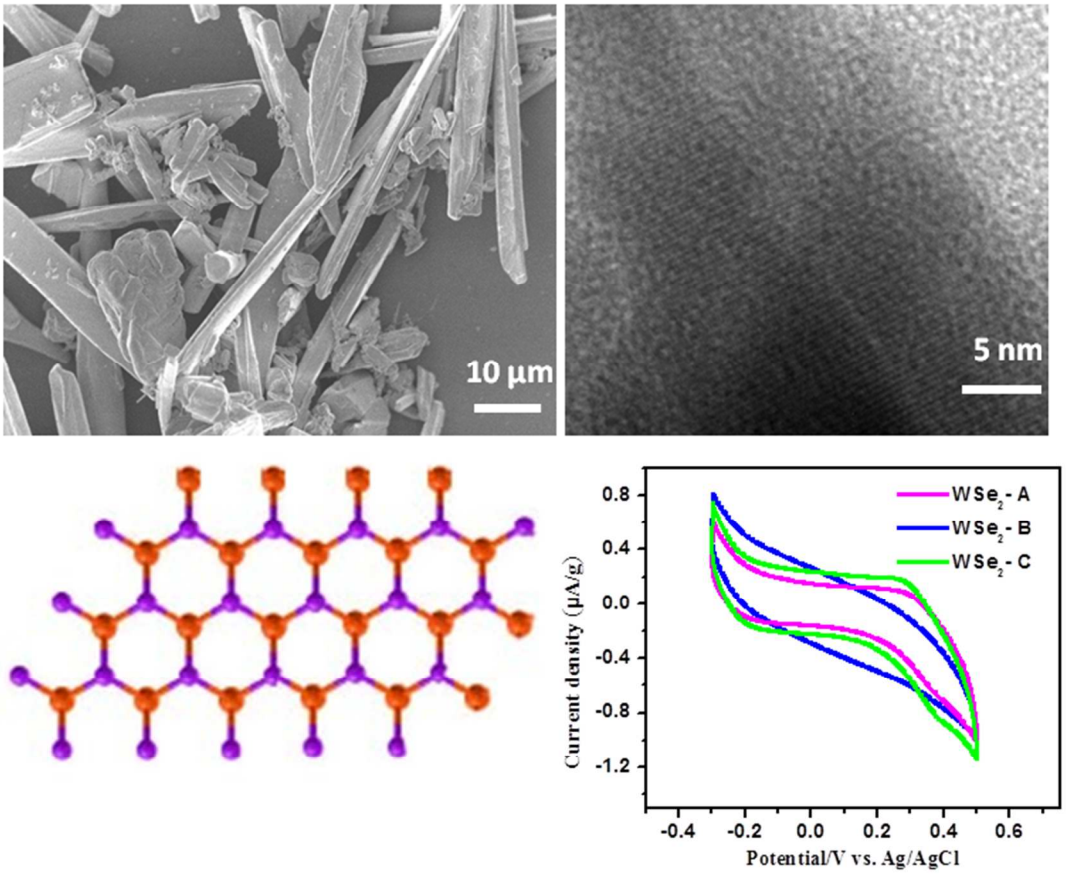

The WSe_2 micro/nanorod prepared using microwave and hydrothermal method shows noteworthy performance towards cyclic stability for supercapacitor. Our results opens new avenue to synthesize various inorganic layered materials using simple one step method for energy storage applications.